Framework for Analyzing the Complex Interactions Between Spacecraft Motion and Slosh Dynamics in Low-G Environments

William J. Elke III (1*), Jing Pei (2), Carlos M. Roithmayr (2), Ryan J. Caverly (1)

(1) University of Minnesota - Twin Cities, (2) NASA Langley Research Center, (*) Corresponding Author

PRESENTED AT:

1. INTRODUCTION

Background

Current and future space exploration missions will utilize spacecraft with a large fuel-to-dry-mass ratio. Large amounts of liquid propellant can lead to significant coupling between the rigid-body dynamics of the spacecraft and the motion of the fuel within its storage tank(s).

Of particular interest for this study are the spacecraft-propellant interactions that take place in a low-g environment. In short, small relative accelerations between the spacecraft and its liquid propellants characterize a low-g environment [1, 2].

There are many ways this interaction can negatively affect system level requirements and mission success. For example, during Apollo missions 8, 10, and 11, the service module (SM) separated from the command module prior to Earth reentry [3, 4]. Crew members onboard the command module observed the jettisoned SM tumbling through their field of view despite the fact that the jettison maneuver was planned in such a way that the service module should have never done so [4]. This potentially catastrophic, unintended retrograde motion is attributed to the gross reorientation of the residual propellant inside the tanks of the SM [3, 4].

Modeling Strategies

Analyzing the complex interaction between a spacecraft and propellant in a low-g environment is a complicated undertaking and active area of research. Examples of approaches taken to modeling this interaction include

- a particle model [4],
- a spring-restrained pendulum [2],
- computational fluid dynamics.

Each modeling methodology has its various trade-offs which must be considered such as tractability and simplicity. The particle model from Ref. [4] appears to be successful in simulating the general motion of the residual propellant inside the tanks and reproducing the observed retrograde motion from Apollo missions 8, 10, and 11. The model desribed in Ref. [4] is used as a framework for the work presented here.

State of the Art

References [4, 5, 8−10] describe modeling approaches based on the particle model. References [8, 9] utilize a sphere of varying radius as opposed to an infinitesimal particle inside a spherical cavity to model the propellant. References [5, 10] utilizes a particle like Ref. [4], however, the constraint surface that the particle moves within has geometry based on the behavior of the propellant in a one-g environment instead of the geometry of the storage tank.

Motivation

An accurate low-g slosh and spacecraft dynamics model that can run in real time or faster has many space guidance, navigation, and control applications such as

- assessing degradation of handling qualities in the presence of low-g slosh dynamics during manual rendezvous proximity operations and docking events,
- improving accuracy of the representation of the dynamics in a spacecraft attitude navigation filter,
- quickly assessing jettison maneuvers to avoid recontact as demonstrated in Refs. [4, 5].

Contribution

The novel contribution of this work is the development of a generalized framework for rapidly analyzing spacecraft-propellant interactions in a low-g environment. The methodology closely follows the particle modeling approach described in Ref. [4] with some additional enhancements—heritage and analytical tractability being the top motivating factors. The authors of this work correct the mistakes found in Ref. [4] and apply the principles of impulse and momentum as a more rigorous approach to the collision dynamics.

Section 2 discusses the dynamics modeled in Ref. [4] and points out the mistakes and unmodeled dynamics discovered upon review. Section 3 contains an overview of the simulation framework and results from an example. Conclusions are presented in Section 4.

3A. SIMULATION FLOW

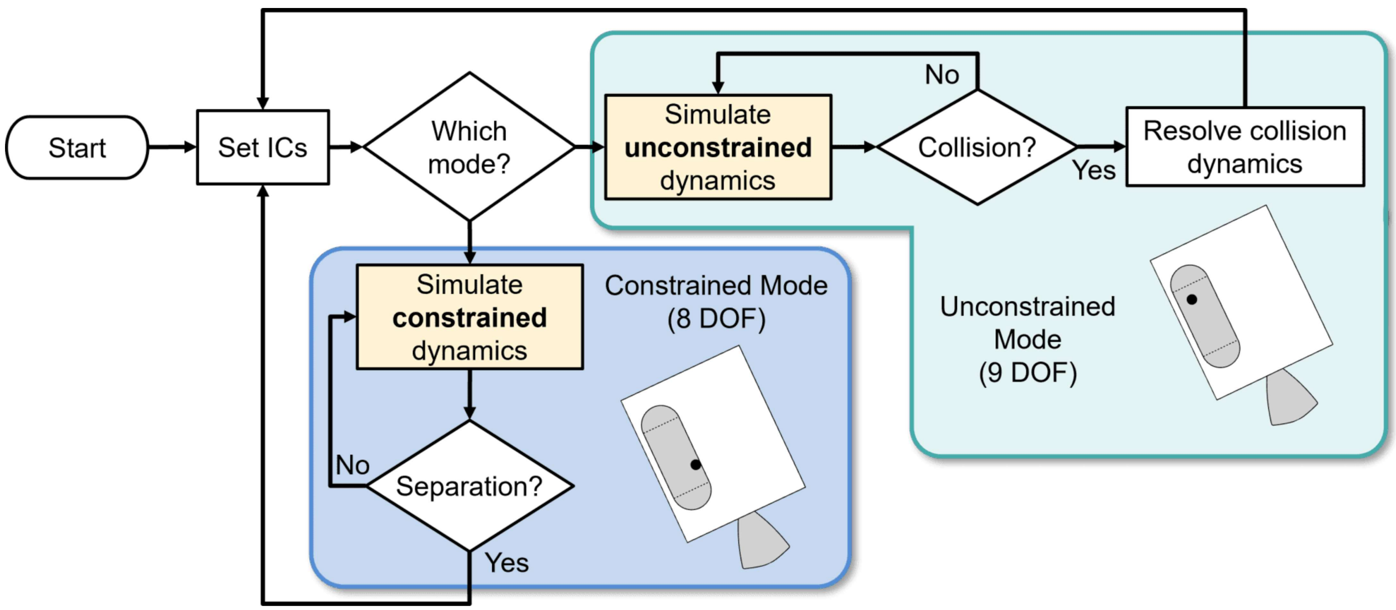

Fig. 2. Block diagram of simulation architecture.

Overview

The simulation framework—based upon the considerations discussed in Section 2—has two operating modes. The Unconstrained Mode is active when the particle moves freely and is not in contact with the tank wall, whereas the Constrained Mode is utilized when the particle slides along the tank wall. Figure 2 provides a flowchart of the simulation architecture. Reference [16] establishes the framework for the enforcement and relaxation of constraints implemented in this work.

Initialization

The simulation begins with initial conditions specified by the user. This includes the spacecraft position, attitude, velocity, and angular velocity, as well as the particle position and velocity. A flag indicating the mode in which the simulation starts is also initialized. Once the initialization is completed, the simulation checks the flag to see if the Unconstrained Mode or Constrained Mode should be used.

Unconstrained Mode

The Unconstrained Mode begins by numerically integrating the 9 DOF unconstrained equations of motion described in Section 2. Simultaneously, it is also continuously checking for a collision between the tank wall and particle. If there is no collision detected, the simulation continues numerical integration of the unconstrained equations of motion. Once a collision has been detected, the value of the states immediately following the collision are computed algebraically using the principles of impulse and momentum described in Section 2, the flag is set to indicate that the Constrained Mode must be activated, and the simulation exits the Unconstrained Mode. The simulation then returns to the beginning of the flowchart where the initial conditions are reset to the values following the collision.

Constrained Mode

The Constrained Mode begins by numerically integrating the 8 DOF constrained equations of motion described in Section 2. Simultaneously, the normal force between the wall and particle is computed at each time step. If the normal force is tensile, then a separation occurs. Otherwise, the simulation continues numerical integration of the states using the constrained equations of motion. Once a separation has been detected the flag is set to indicate that the Unconstrained Mode must be activated. The simulation then exits the Constrained Mode and returns to the beginning of the flowchart where the initial conditions are reset to the states at the time step immediately preceding the separation.

The exchange between the Unconstrained and Constrained Modes continues until the user-specified terminal simulation time is reached.

3B. NUMERICAL EXAMPLE

[VIDEO] https://res.cloudinary.com/amuze-interactive/video/upload/vc_auto/v1661281305/iaf/E8-88-41-82-39-E0-D4-05-F4-64-0C-0F-82-AA-6C-4A/Video/animation_IC_v9_fps_30_nwfafl.mp4

Fig. 3. Comparison between the trajectories of spacecraft with and without fuel slosh (left); motion of the particle within the tank of the spacecraft with fuel slosh (right).

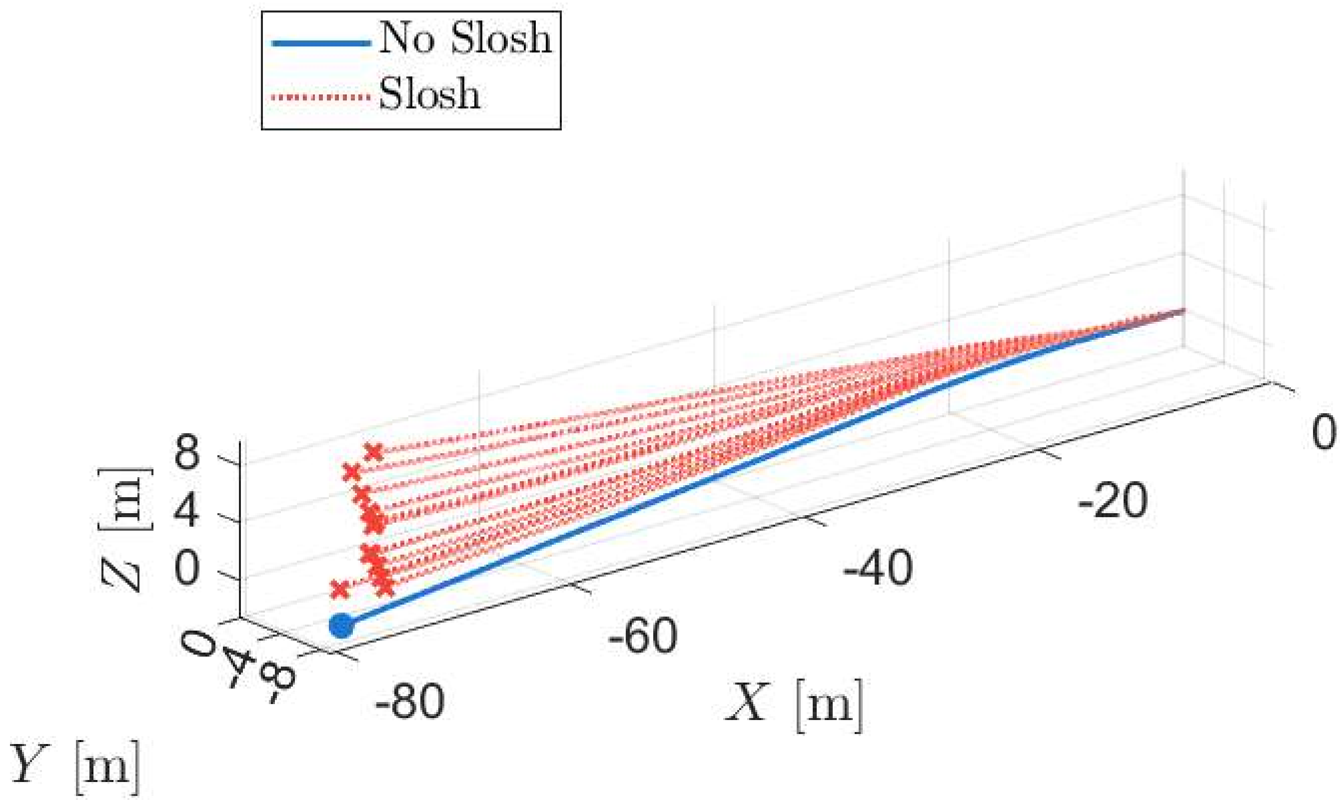

Fig. 4a. Three-dimensional time histories of $B*$.

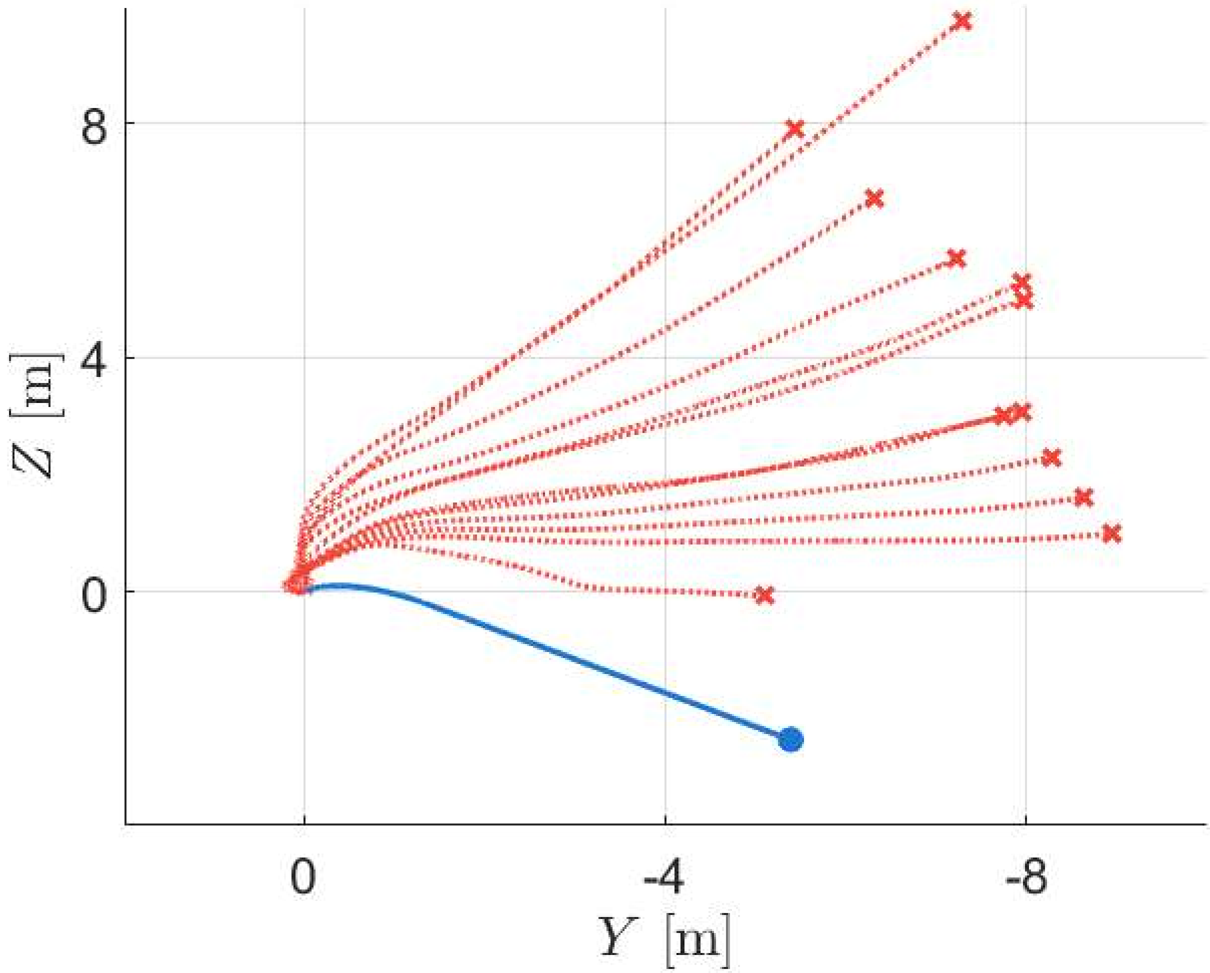

Fig. 4b. Projection of Fig. 4a onto the YZ plane. Positive *X* goes into the figure.

Example Setup

An example is presented that demonstrates simulation capabilities. This notional example involves a stationary spacecraft with an initial angular velocity and a prescribed open-loop thrust profile lasting 30 seconds. Fig. 1 presents a schematic of the system at t = 0 s for a single case. The simulation is run multiple times, with varying conditions of the particle. This is done to highlight the effects fuel slosh can have on the motion of the spacecraft in a low-g environment.

The spacecraft in the simulation has the same mass properties as the service module in Ref. [4], but has only one domed tank instead of two. The spacecraft is stationary at t = 0 s and has an initial angular velocity in the *x* direction of 18 deg/s. The spacecraft follows a thrust profile that begins with the reaction control system thrusters firing in the negative *x* direction at t = 0 s; the thrusters shut off at t = 15 s. The thruster dynamics are not modeled and the resultant force, $\underset{\rightarrow}{F}$, and moment, $\underset{\rightarrow}{M}$, are applied at B^*. The center of mass of the spacecraft is not located on the *x* axis, as seen in Fig. 1, which is consistent with the configuration provided in Ref. [4].

Results

A comparison between a spacecraft with and without the fuel slosh is shown in Fig. 3.

The resulting trajectories can be seen in Fig. 4. Figure 4a shows a three-dimensional view of the time history of the position of $B*$. The solid blue line represents the no-slosh case, whereas the dashed red lines represent cases with various initial positions and velocities of the particle. The initial velocities of the particle have magnitudes in the range 0 to 11 in/s. Figure 4b shows the projection of the trajectories onto the YZ plane.

The ensemble of trajectories after 30 seconds shown in Fig. 3b demonstrates the importance of capturing the interactions between fuel slosh and spacecraft. For the assumed parameters and open-loop thrust profile, deviations in the final position of $B*$ can be as much as 10 m in magnitude. A review of the system's energy and momenta verified the validity of the equations of motion. The system's energy increases when the thrusters are on and conserved when the thrusters are off, provided no collisions occur. The system experiences discrete energy losses whenever a collision occurs. The system's translational and angular momenta are conserved when the thrusters are off but are not conserved when the thrusters are on.

2. DYNAMICAL FEATURES

System Description

The present work bases its modeling methodology on a modified form of the dynamical system found in Ref. [4]. The main features of this system include

- a spacecraft treated as rigid-body with constant mass and inertia properties,
- a single cylindrical tank capped with hemispheres tanks referred to as "domed tanks,"
- propellant treated as an infinitisemal particle with mass equal to the residual propellant,
- perfectly inelastic collisions between the particle and tank wall,
- frictionless interactions between the bodies.

Figure 1 presents a schematic of the system where the center of mass of the spacecraft is denoted by Point $B*$ and the particle is denoted as Point P. Note that Point $B*$ does not necessarily lie along the centerline of the spacecraft and that the particle is infinitesimal despite the size of Point P.

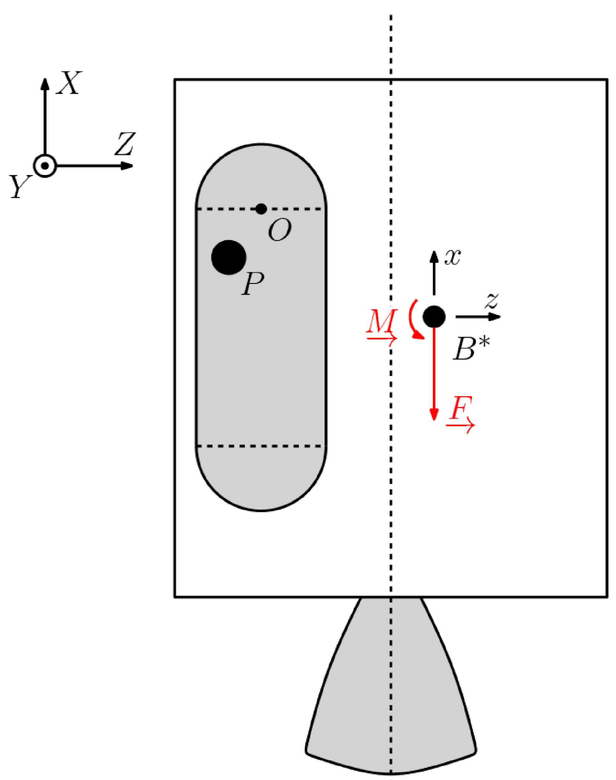

Fig. 1. Schematic of the spacecraft and particle system.

Equations of Motion

Reference [4] derives the translational and rotational equations of motion of the spacecraft via a Newton-Euler approach. Subsequently, the translational acceleration of the particle is derived using kinematics. The derivation of the translational acceleration of the particle contains some errors; specifically, there are missing terms in Eqns. (10)−(14) of Ref. [4].

These missing terms are a result of an incorrect application of the transport theorem [14, 15]. Consider an inertial reference frame, Frame *i*, body-fixed reference frame, Frame *b*, and particle tracking reference frame, Frame *e*. The transport theorem applied to the angular velocity of Frame *b* relative to Frame *i* is

$$\underset{\rightarrow}{\omega}^{bi^{\bullet b}} = \underset{\rightarrow}{\omega}^{bi^{\bullet e}} + \underbrace{\underset{\rightarrow}{\omega}^{eb} \times \underset{\rightarrow}{\omega}^{bi}}_{\text{Missing}}.$$

The crucial transport term is left out of Ref. [4] resulting in the omission of the term labeled as "Missing." It appears the authors of Ref. [4] simply set $\underset{\rightarrow}{\omega}^{bi^{\bullet b}} = \underset{\rightarrow}{\omega}^{bi^{\bullet e}}$ and did not account for the fact that Frame *e* can rotate relative to Frame *b*. This mistake results in incorrect equations of motion of the particle and effects that permeate throughout the entire model.

Constraints

When the particle is moving along the tank wall, a kinematic constraint is enforced to keep it from passing through the tank wall and the number of degrees of freedom (DOF) are reduced from 9 DOF to 8 DOF.

Collision Dynamics

A collision occurs when the particle makes initial contact with the tank wall. The collision implementation described in Ref. [4] involves first solving the constrained kinematic equation for the acceleration of the particle at the moment of the collision. Using the result from the first step, normal forces having equal magnitudes and opposite directions are computed and applied to the spacecraft and particle. The consequences of the mistake in the equations of motion manifest here. Since the first step involves solving the equations of motion, the resulting forces are incorrect.

There is no evidence in Ref. [4] that the principles of impulse and momentum were considered for the full scope of the DOF involved. Therefore, it is unclear whether the behavior of the system would be accurate even with correct equations. These principles are applied in this work and can be found in Refs. [14, 15].

The corresponding paper contains a complete description of the dynamics discussed here and the audience is encouraged to read it for more information.

4. CONCLUSIONS

Conclusions

A framework for predicting the complex interactions between fuel slosh and spacecraft in a low-g environment is described in this paper along with historical context. The study is motivated by the methodology developed during Project Apollo as engineers sought to predict the unintended retrograde motion displayed by the service module following separation from the command module, prior to Earth reentry. Detailed contractor reports of the simulation are lost; thus, in this work, the authors were able to recreate the system dynamics from first principles based on the limited information provided in Ref. [4]. Along the way, several mistakes were identified in Ref. [4] and presented here. The contemporary simulation flowchart is discussed and results from an example application are presented. Results highlight the effects liquid propellant can have on the gross motion of a spacecraft in a low-g environment. The simulation framework presented in this study serves as a platform for analyzing the underlying dynamics behind that complex interaction.

Contact information of the authors is provided with this iPoster. Please reach out if there are any questions or discussions to be had.

Acknowledgements

This material is based upon work supported by the NASA Office of STEM Engagement (OSTEM) under Grant No.80NSSC19K1672 issued through the NASA Fellowships Program under MUREP funding.

AUTHOR INFORMATION

William J. Elke III

Graduate Student

Department of Aerospace Engineering and Mechanics

University of Minnesota - Twin Cities

Jing Pei

Aerospace Engineer

Atmospheric Flight & Entry Systems Branch

NASA Langley Research Center

Carlos M. Roithmayr

Aerospace Engineer

Vehicle Analysis Branch

NASA Langley Research Center

Ryan J. Caverly

Assistant Professor

Department of Aerospace Engineering and Mechanics

University of Minnesota - Twin Cities

ABSTRACT

The fuel-to-dry-mass ratio of spacecraft continues to grow as new human spaceflight missions target destinations afrom Earth. Large amounts of liquid propellant can lead to significant coupling between the rigid-body dynamics of the spacecraft and the motion of the fuel within its storage tank. The present work gives an overview of the dynamic features and a flowchart for a method of simulating the motion of a spacecraft with fuel slosh inside a cylindrical, domed tank in a low-g environment. The method involves modeling the liquid propellant as a particle that transfers momentum to the spacecraft through perfectly inelastic collisions with the tank wall. The foundation of the modeling methodology is the approach taken during the Apollo program used to predict the effect of fuel slosh on the complex motion exhibited by the Service Module following separation from the Crew Module. This paper discusses the motivation, methodology, and conclusions from the Apollo-era method, and subsequently builds upon it by incorporating corrections to the derivation of the dynamics and filling in the gaps due to unavailability of the detailed contractor report and simulation code. The results presented in this paper provide an example that demonstrates the effect that fuel slosh can have on the trajectory of a spacecraft in a low-g environment.

REFERENCES

[1] F. T. Dodge, *The New "Dynamic Behavior of Liquids in Moving Containers,"* Southwest Research Institute, 2000.

[2] P. J. Enright and E. C. Wong, "Propellant Slosh Models for the Cassini Spacecraft," Astrodynamics Conference, pp. 186–195, 1994.

[3] "MSC-03466, Apollo 11 Mission Anomaly Report No. 3, Service Module Entry, November 1970," NASA Apollo 11 Technical Crew Debriefing, vol. II, Jul. 1969.

[4] D. H. Merchant, R. M. Gates, and J. F. Murray, "Prediction of Apollo Service Module Motion after Jettison," Journal of Spacecraft and Rockets, vol. 8, pp. 587–592, 1971.

[5] P. G. Good, A. Carpenter, H. Flanders, and T. Gardner, "STARDUST TCM and Despin in the Presence of Complex Fuel Dynamics," Advances in the Astronautical Sciences, vol. 99, pp. 611–628, Feb. 1998.

[6] F. T. Dodge, S. T. Green, and D. D. Kana, "Fluid Management Technology: Liquid Slosh Dynamics and Control," NASA-CR-189107, Nov. 1991.

[7] J. W. Jang, A. Alaniz, L. Yang, J. Powers, and C. Hall, "Mechanical Slosh Models for Rocket Propelled Spacecraft," AIAA Guidance, Navigation, and Control (GNC) Conference, Aug. 2013.

[8] J. P. B. Vreeburg, "Dynamics and Control of a Spacecraft with a Moving Pulsating Ball in a Spherical Cavity," Acta Astronautica, vol. 40, pp. 257–274, 1997.

[9] J. P. Vreeburg and D. J. Chato, "Models for Liquid Impact Onboard Sloshsat FLEVO," AIAA Space Conference and Exposition, Sep. 2000.

[10] Z. Zhou and H. Huang, "Constraint Surface Model for Large Amplitude Sloshing of the Spacecraft with Multiple Tanks," Acta Astronautica, vol. 111, pp. 222–229, 2015.

[11] R. Gates and D. Merchant, "General Motion of a Rigid Spacecraft with Fluid Reorientation—Theoretical Manual," D2-118301-1, The Boeing Co., Houston, Texas, May 1970.

[12] J. Murray, "General Motion of a Rigid Spacecraft with Fluid Reorientation—Computer User's Manual," D2-118301-2, The Boeing Co., Houston, Texas, May 1970.

[13] D. Merchant and R. Gates, "CM-SM Separation Dynamics," 5-2961-HOU-107, The Boeing Co., Houston, Texas, Dec. 1969.

[14] T. R. Kane and D. A. Levinson, *Dynamics: Theory and Applications*, McGraw-Hill, 1985.

[15] A. V. Rao, *Dynamics of Particles and Rigid Bodies*, Cambridge University Press, 2006.

[16] S. Djerassi, "Imposition of Constraints," Journal of Applied Mechanics, vol. 61, pp. 434–439, Jun. 1994.